
INTERAURAL COHERENCE ACROSS FREQUENCY CHANNELS ACCOUNTS FOR BINAURAL DETECTION IN COMPLEX MASKERS

A PREPRINT

Bernhard Eurich

Department für Medizinische Physik und Akustik
Universität Oldenburg
26111 Oldenburg, Germany
bernhard.eurich@uni-oldenburg.de

Jörg Encke

Department für Medizinische Physik und Akustik
Universität Oldenburg
26111 Oldenburg, Germany

Stephan D. Ewert

Department für Medizinische Physik und Akustik
Universität Oldenburg
26111 Oldenburg, Germany

Mathias Dietz

Department für Medizinische Physik und Akustik
Universität Oldenburg
26111 Oldenburg, Germany

October 7, 2021

ABSTRACT

Differences in interaural phase configuration between a target and a masker can lead to substantial binaural unmasking. This effect is decreased for masking noise having an interaural time difference (ITD). Adding a second noise with the opposite ITD further reduces binaural unmasking. Thus far, simulation of the detection threshold required both a mechanism for internal ITD compensation and an increased binaural processing bandwidth. An alternative explanation for the reduction is that unmasking is impaired by the lower interaural coherence in off-frequency regions caused by the second masker (Marquardt and McAlpine 2009, JASA pp. EL177 - EL182). Based on this hypothesis the current work proposes a quantitative multi-channel model using monaurally derived peripheral filter bandwidths and an across-channel incoherence interference mechanism. This mechanism differs from wider filters since it is moot when the masker coherence is constant across frequency bands. Combined with a monaural energy discrimination pathway, the model predicts the differences between single- and double-delayed noise, as well as four other data sets. It can help resolving the inconsistency that simulation of some data sets requires wide filters while others require narrow filters.

1 Introduction

The detection of a pure tone in noise is facilitated by differences in the interaural phase between tone and noise (Hirsh, 1948). The improvement in the detection threshold compared to the diotic case is referred to as the binaural masking level difference (BMLD). The maximum BMLD is observed when detecting an antiphasic pure tone target (S_π) in an in-phase noise masker (N_0). Adding an interaural time difference (ITD = Δt) to the masker has been observed to reduce the BMLD (Langford and Jeffress, 1964). Explanations of the underlying interaural mechanisms have referred to the normalized cross-correlation function. For two complex-valued signals $u(t)$ and $z(t)$ of the form $u(t) = a(t) e^{i\omega(t)}$ and $z(t) = a(t) e^{i\omega(t)}$, where $a(t)$ is the instantaneous amplitude and $\omega(t) = 2\pi f(t)$ the instantaneous angular frequency, it is defined as

$$\gamma(\tau) = \frac{\int_{-\infty}^{\infty} u^*(t)z(t+\tau)dt}{\sqrt{E_u E_z}}. \quad (1)$$

E_u and E_z denote the energies of the signals, i.e., $E_u = \int_{-\infty}^{\infty} |u(t)|^2 dt$, and the asterisk the complex conjugate. The real part is the real-valued correlation function $\rho(\tau)$ which is also that which (1) delivers for real-valued signals, such as

sound pressure. The values at $\tau = 0$ are referred to as correlation coefficients and written in the short forms γ and ρ , respectively. Models evaluating the real-valued correlation coefficient ρ explain BMLD as a function of Δt (Rabiner et al., 1966) and partial correlation obtained by mixing correlated and uncorrelated noise (Robinson and Jeffress, 1963) well, but only for the special case where $\rho = |\gamma|$, i.e. if the real-valued correlation function $\rho(\tau)$ has a (main or side) peak at $\tau = 0$.

The modulus $|\gamma(\tau)|$ can be described as the envelope of $\rho(\tau)$ and provides a measure for the phase consistency between the two signals $u(t)$ and $z(t + \tau)$. We refer to it as the temporal coherence function and at $\tau = 0$ to the interaural coherence $|\gamma| = |\gamma(\tau = 0)|$ (see Encke and Dietz 2021 for an in-depth discussion and visualization).

If $u(t) = z(t)$, i.e. auto- instead of cross-correlation, $|\gamma(\tau)|$ is determined by the signal bandwidth (Wiener-Khinchin theorem, Khintchine, 1934). In the auditory context, the signal bandwidth is the bandwidth after peripheral filtering. Langford and Jeffress (1964), Rabiner et al. (1966) and Encke and Dietz (2021) have shown that the ITD dependence of the BMLD can to a large extent be explained based on $\gamma(\tau)$, if a basilar membrane mimicking filter with a bandwidth according to Glasberg and Moore (1990) has been applied to the signal.

Other models rely on the hypothesis of Jeffress (1948) stating that the binaural system is able to compensate for the interaural masker delay Δt by internal delays, referred to as delay lines (van der Heijden and Trahiotis, 1999; Stern and Shear, 1996; Bernstein and Trahiotis, 2018, 2020). That is, the brain has access to the real-valued cross-correlation function over a considerable range of latency differences. To account for the decrease in BMLD with increasing Δt , delay-line-based models reasonably assume a decreasing accuracy of the delay compensation, described by a $p(\tau)$ function (e.g. Colburn, 1977).

van der Heijden and Trahiotis (1999) introduced a new stimulus, aiming to isolate the additional unmasking facilitated by putative delay lines in addition to any unmasking resulting from a possible partial correlation at $\tau = 0$. First, they measured detection thresholds for a 500 Hz pure tone masked by broadband noise as a function of the ITD Δt (single-delayed noise, SDN; rectangles in Figures 1d). This condition is equivalent to Langford and Jeffress (1964, their Figures 1 and 2) and the corresponding BMLDs are very similar. They further generated a stimulus called double-delayed noise (DDN, diamonds in Figures 1d) by adding two noises, one with a positive and one with a negative ITD. For any given Δt the conventional SDN and DDN have the same correlation coefficient. The DDN, however, limits the usefulness of the putative delay lines as internal delays can only compensate for the ITD of one noise. van der Heijden and Trahiotis (1999) therefore used the decline of BMLD with Δt in DDN to derive the binaural processing bandwidth. As outlined above, the two quantities are connected by the Wiener-Khinchin theorem. The term "binaural processing bandwidth" is used to leave open the possibility that this bandwidth differs from the respective basilar membrane filter characteristics, e.g., by some form of spectral integration in the binaural pathway. In contrast to previous attempts using SDN for processing bandwidth estimates (Langford and Jeffress, 1964; Rabiner et al., 1966), van der Heijden and Trahiotis (1999) could be sure that their calculation was not confounded by a more gradual BMLD decline caused by delay lines. That is, they prevented a potential underestimation of the processing bandwidth. In a final step, van der Heijden and Trahiotis (1999) attributed the larger BMLD in SDN, compared to DDN, to the correlation increase caused by the delay line (as illustrated by the dashed arrow in Figure 1d). To fit their model to the data, they (1) adjusted the filter bandwidth to account for the DDN thresholds and then (2) derived a $p(\tau)$ function so that the predetermined filter bandwidth plus delay line accounted for the SDN thresholds. The peripheral filter that best fit their model to the data had an equivalent rectangular bandwidth (ERB) of 130 to 180 Hz at 500 Hz. This bandwidth range is consistent with estimates from binaural notched-noise experiments (e.g. Sondhi and Guttmann 1966, Kolarik and Culling 2010). It does, however, not agree with SDN data fitted for different masker bandwidths by Bernstein and Trahiotis (2020). There, despite the very similar method, an ERB of "not greater than 100 Hz" (for the filter centered on-frequency, i.e. at 500 Hz) was required. This narrow processing bandwidth is in agreement with processing bandwidths obtained with SDN and without considering delay lines, which are 50...100 Hz (Rabiner et al., 1966; Langford and Jeffress, 1964; Dietz et al., 2021). For comparison, "standard", monaurally obtained ERBs at 500 Hz center frequency are 79 Hz (Glasberg and Moore, 1990).

Marquardt and McAlpine (2009) pointed out that the thresholds obtained with spectrally complex maskers, particularly with DDN, are not necessarily caused by a large peripheral filter bandwidth. They noted that the interaural coherence of SDN is fairly constant across frequency bands (see Figure 1a,c) while the coherence in DDN is spectrally modulated (Figure 1b,c). Its spectral shape is derived in the appendix. Depending on Δt , the off-frequency coherence can thus be lower in DDN than in SDN while the on-frequency coherence is identical in both stimulus types. Marquardt and McAlpine (2009) hypothesized that "reduced interaural coherence appears detrimental to binaural detection, even outside the target's frequency channel". If this is true, both SDN and DDN thresholds can potentially be explained using the same standard filter bandwidth with the lower off-frequency coherence elevating the corresponding DDN thresholds. Such a standard-filter-plus-off-frequency-impact concept implies that the gradual unmasking decline in

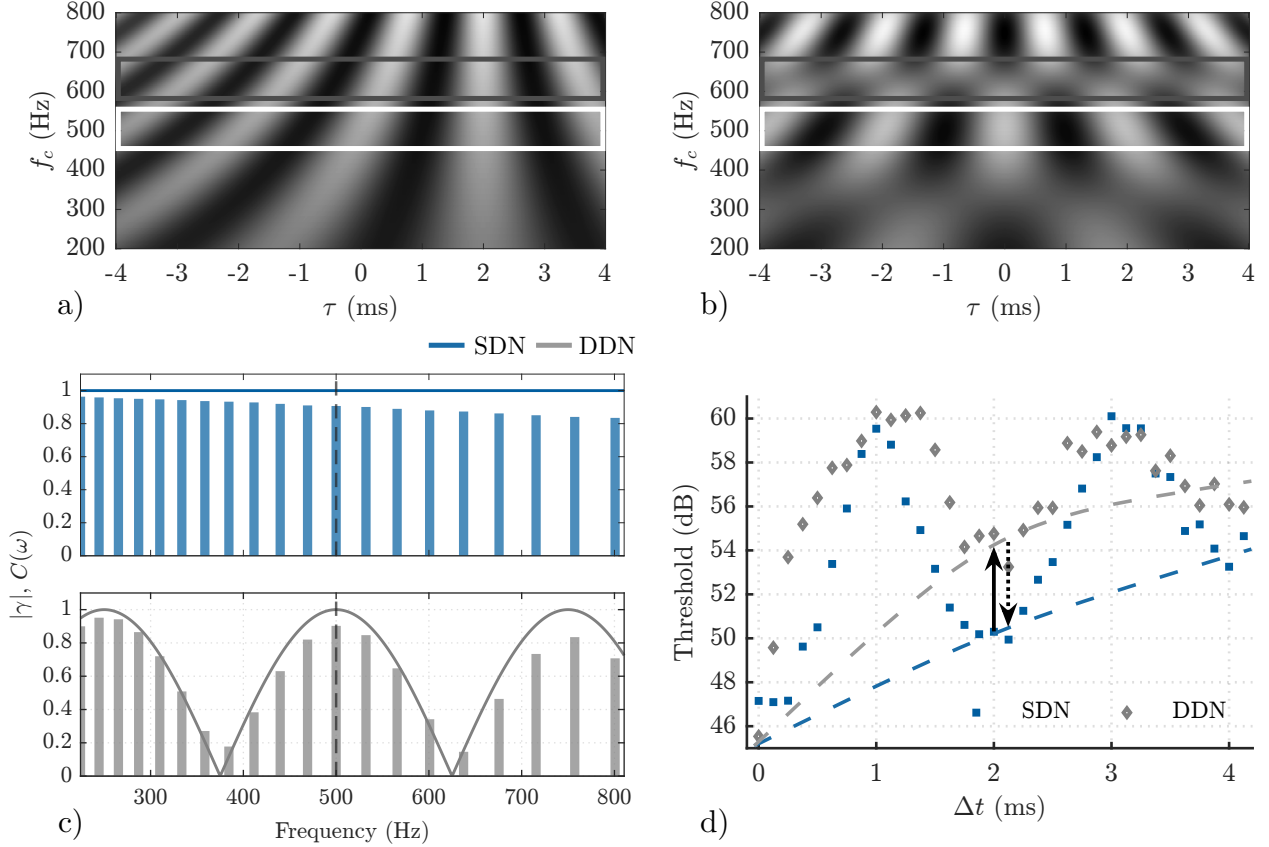


Figure 1: Panel **a)** Cross-correlogram of SDN with $\Delta t = 2$ ms. White and black areas represent maxima and minima of the cross-correlation functions, respectively. The white box highlights the 500 Hz frequency channel while the gray box highlights a channel centered at 625 Hz. **b)** Interaural cross-correlogram as in a) but for DDN. **c)** Continuous lines: Normalized Cross-power spectral density (CPSD) at $\Delta t = 2$ ms as a function of frequency, $|C(\omega)|$, as derived in (13) et seq.; Bars: Interaural coherence $|\gamma|$ of the signals after peripheral Gammatone filtering. **d)** Thresholds of S_π detection in SDN and DDN as a function of interaural delay Δt from van der Heijden and Trahiotis (1999). The dashed lines symbolize the coherence-decline induced threshold increase determined by a processing bandwidth of ERB = 79 Hz (lower line) and for an ERB = 130 Hz (upper line). As denoted by the arrows, the data can be explained in two ways: (1: continuous arrow) The DDN thresholds are determined by the cross-correlation function at 500 Hz and a processing bandwidth ≥ 130 Hz. A delay line causes the lower SDN thresholds. (2: dotted arrow) The SDN thresholds are determined by the ITD-dependent coherence as derived from an ERB of 79 Hz. Off-frequency incoherence in DDN causes higher DDN thresholds.

SDN does not have to originate from delay lines because it is already explained by the coherence that is defined by the narrow filtered signal.

The concept of a detrimental incoherence interference may also help in reducing inconsistencies in estimating the processing bandwidth from other binaural detection experiments, e.g., band-widening versus notched-noise (Nitschmann and Verhey, 2013). This concept may enable models to account for the different stimulus types with a fixed standard filter bandwidth and without delay lines. Thus far, however, the hypothesis has only been tested using a very simplistic model. The simulations from Marquardt and McAlpine (2009) with an S_0 target lack adequate precision and there are no simulations for the S_π target.

The goal of the present study was a model based on the standard-filter-plus-off-frequency-impact concept that can account for the critical van der Heijden and Trahiotis (1999) data, with an accuracy comparable to the wider-filter-plus-delay-line model by van der Heijden and Trahiotis (1999). This would resolve the present contradiction that filters need to be narrow to account for some and broad to account for other data.

The proposed model follows the approach of Encke and Dietz (2021) that the coherence $|\gamma|$ is responsible for the binaural system's unmasking capabilities. A low coherence expresses itself in fluctuations in the interaural phase difference (IPD). The hypothesized across-channel incoherence interference is implemented in analogy to different currents in a bundle of electric cables: An alternating, i.e. fluctuating, current causes electromagnetic interferences, while direct current does not. In the frame of IPD fluctuations, this means: Only frequency channels carrying less-coherent signals, i.e. stronger IPD fluctuations, affect the on-frequency channel. We evaluated our model with data from five different studies in three groups:

- (1) van der Heijden and Trahiotis (1999) combined all key aspects required to revisit Marquardt and McAlpine's hypothesis: (a) The SDN thresholds are planned to be determined by the decay of $|\gamma|$ with a 79 Hz-wide Gammatone filter. (b) The higher DDN thresholds will be simulated by an across-channel incoherence interference but with the same 79 Hz on-frequency filter. The most important datapoints to judge this are at those ITDs where the on-frequency coherence of SDN and DDN is the same, but thresholds differ. For S_0 detection this is the case at $\Delta t = 1$ ms and 3 ms, for S_π detection at $\Delta t = 2$ ms and 4 ms.
- (2) Marquardt and McAlpine (2009) not only presented the above-mentioned hypothesis but also detection thresholds with SDN and DDN maskers that are spectrally surrounded by constant-IPD bands that either do or do not cause interaural incoherence at the transitions. Their reported differences impose a challenge for single-channel models that use a constant filter bandwidth.
- (3) Sondhi and Guttman (1966); Holube et al. (1998); Kolarik and Culling (2010), reported detection thresholds of an S_π tone centered in an in-phase noise that is spectrally surrounded by antiphase noise. These simulations are included for an additional discussion about the proposed narrow-filter-plus-channel-interaction concept, since larger binaural processing bandwidths have previously been derived based on such data.

2 Description of the Model

Figure 2 shows the processing stages of the proposed model. It is designed as a multi-channel model through all stages, but these were here realized and tailored to predict binaural-detection data with a 500 Hz pure-tone target. Briefly, the model builds on the analytical single-channel model approach of Encke and Dietz (2021). Furthermore, the model includes an across-channel interaction mechanism. It consists of a multi-channel binaural processing pathway and a monaural pathway. Both pathways compare multiple tokens of the processed signal representation of the condition-specific masker to the representation of signal plus masker. This comparison has been suggested to mimic a subject's strategy of comparing a stimulus to a learned reference template (Dau et al., 1996, 1997; Jepsen et al., 2008; Breebaart et al., 2001a; Bernstein and Trahiotis, 2017). Based on these comparisons, both pathways deliver a sensitivity index (d'). An optimal combination of the pathways' estimates gives the overall d' estimate of the model (Biberger and Ewert, 2016).

2.1 Peripheral Processing

The left and right input signals were processed with a fourth-order Gammatone filterbank that represents basilar-membrane bandpass filtering. The filterbank implementation by Hohmann (2002) was employed with a spacing of five filters per ERB in the range of 67 Hz to 1000 Hz. The grid was defined by centering one filter at 500 Hz. This filter had an ERB of 79 Hz (Glasberg and Moore, 1990) and was indexed with $k = 0$.

In order to focus on the influence of the above-mentioned key elements, the present implementation did not include any other peripheral processing such as low-pass filtering, power-law compression, or half-wave rectification.

2.2 Binaural Pathway

Right at the outset the correlation coefficient $\gamma(\tau = 0) = \gamma$ was derived from the analytical, i.e. complex-valued left and right signals $u(t)$ and $z(t)$ in the frequency channel k , provided by the Gammatone filterbank:

$$\gamma_k = \frac{\overline{u_k(t)z_k(t)^*}}{\sqrt{|\overline{u_k(t)}|^2 |\overline{z_k(t)}|^2}} \quad (2)$$

where $\overline{\bullet}$ marks the temporal mean. This is a more efficient implementation of the definition in 1. The complex-valued correlation coefficient was used because it conveniently combines information about both the mean IPD as $\arg\{\gamma\}$ and about IPD fluctuations, i.e. interaural coherence $|\gamma|$. Theoretically this information can be extracted from two (real-valued) correlation units, ideally with 90° IPD-tuning difference (Dietz and Ashida, 2021). As discussed in Encke

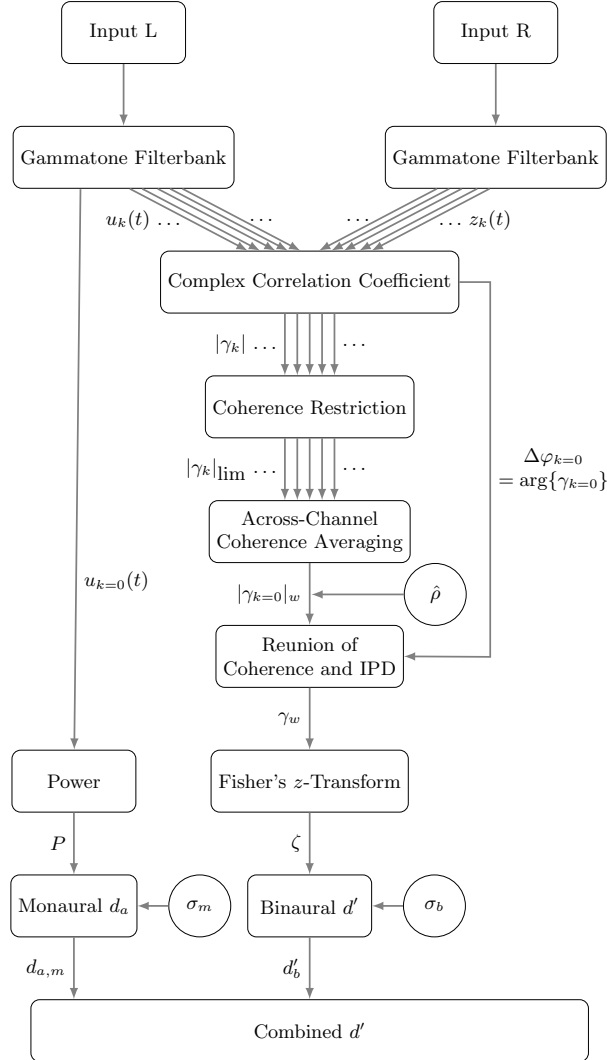


Figure 2: Processing stages of the proposed model. See main text for details.

and Dietz (2021), this is meant to represent the ensemble information of binaural neurons in mammals (McAlpine et al., 2001; Grothe et al., 2010), including their sensitivity to fast fluctuations (Siveke et al., 2008; Joris et al., 2006; van der Heijden and Joris, 2010). Sensitivity to the amount of IPD fluctuations makes this model class crucially different from most established models of binaural unmasking, where real-valued correlation is used (Bernstein and Trahiotis, 2017; van der Heijden and Trahiotis, 1999) which only depends on time-averaged IPDs or ITDs.

As pointed out in the Introduction, the novelty of the present model is the interference of IPD fluctuations across frequency channels. The term incoherence interference describes purely detrimental effects, i.e. only channels with lower coherence affect their neighbor, but not the other way around. Simulation therefore involves a *restricted* across-channel weighted average of the coherence $|\gamma|_k$: The $|\gamma|_k$ are limited to the coherence of the channel for which the post-interference coherence $|\gamma|_w$ is calculated, thus referred to as $|\gamma|_{k,\text{lim}}$.

$$|\gamma|_w = \sum_{-m}^m w(k) |\gamma|_{k,\text{lim}} \quad (3)$$

where $w(k)$ symbolizes a function that weights the contribution of a channel k to the resulting $|\gamma|_w$. The employed weighting function has an exponential decay described by

$$w(k) = e^{-|k|/(b\sigma_w)}. \quad (4)$$

σ_w represents the decay parameter, normalized by the number of filters per ERB, b . The double-exponential decay shape is an ad-hoc choice, inspired by descriptions of the channel interaction through spread of excitation in cochlear implants (Bingabré et al., 2008; Biesheuvel et al., 2016).

For a low masker coherence, or at the – practically irrelevant – case of a positive SNR, adding a target with an IPD of π relative to the masker can swap the mean IPD from the masker to that of the target. In special cases, the masker alone and masker plus target can have the same coherence, but differ in their mean IPD and thus in their correlation. Thus, the interaural coherence $|\gamma|$ is not sufficient as a decision variable. Instead, γ , including both coherence and the mean IPD, is required. Therefore, the original mean IPD is now "given back" to the coherence after the interference and limitation stage, so that the model can operate on the *complex* correlation coefficient as suggested by Encke and Dietz (2021).

$$\gamma_w = |\gamma|_w e^{\arg\{\gamma_0\}} \quad (5)$$

Unity-limited measures such as coherence- or correlation can be Fisher z , i.e. atanh-transformed to approximate an equal-variance axis in perception (McNemar, 1969, as often applied in psychophysics, e.g., Lüdemann et al., 2007; Bernstein and Trahiotis, 2017, and technical applications, e.g., Just and Bamler, 1994). As in Encke and Dietz (2021), γ_w is multiplied by a model parameter $\hat{\rho} < 1$ to avoid an infinite sensitivity to deviations from a coherence of one. This is equivalent to adding uncorrelated noise to the two input signals. The decision variable of the binaural pathway is thus

$$\zeta = z[\hat{\rho}\gamma_w] \quad (6)$$

where $z[\bullet]$ is the fisher-z transform applied to the modulus of γ_w while leaving the argument unchanged.

In the signal detection stage, the d' is obtained based on the difference between the ensemble averages of the representations of the noise alone, ζ_N , and the representations of the target signal plus noise, ζ_{S+N} :

$$d'_b = \frac{|\zeta_N - \zeta_{S+N}|}{\sigma_b} \quad (7)$$

The internal noise σ_b defines the absolute performance of the binaural model pathway (Encke and Dietz, 2021).

2.3 Monaural Pathway

For the monaural pathway, the power P of the on-frequency filter channel was evaluated. It is half the squared mean of the envelope across the whole signal duration (Biberger and Ewert, 2016). The envelope is the modulus of the complex-valued filter output:

$$P = \frac{|\overline{u_0(t)}|^2}{2} \quad (8)$$

In the stimuli employed in this study, the power is identical in the left and right channels, thus it is sufficient to evaluate only one side.

The d_a for the monaural detection follows the unequal variance model of signal detection theory (Simpson and Fitter, 1973; Swets, 1986) with the averages, μ , and the standard deviations, σ , of each stimulus' P of signal plus masker or masker alone, respectively:

$$d_{a,m} = \frac{\mu_{S+N} - \mu_N}{\sqrt{0.5(\sigma_{S+N}^2 + \sigma_N^2)}}, \mu_{S+N} > \mu_N. \quad (9)$$

The processing accuracy of a signal-induced power change is limited by a model parameter that represents a stimulus-dependent internal noise with a Gaussian distribution of amplitudes and a variance of σ_m^2 . The d_a of the monaural path is therefore

$$d_a = \frac{A - 1}{\sqrt{0.5\sigma_m^2(A + 1)}} \text{ with } A = \frac{\mu_{S+N}}{\mu_N}. \quad (10)$$

2.4 Detector

The sensitivity indices of the binaural, d'_b , and monaural pathway, $d_{a,m}$ were combined in an optimal manner, as in Ewert and Dau (2000); Furukawa (2008); Biberger and Ewert (2016). This assumed two independent indices. The output of the model is thus

$$d'_{b+m} = \sqrt{d'_b^2 + d_{a,m}^2}. \quad (11)$$

The d' that corresponds to the experiment-specific detection thresholds was obtained via table-lookup (Numerical evaluation in Hacker and Ratcliff 1979). This depends on the number of intervals, as well as the down-up-paradigm of the alternative-forced-choice (AFC) procedure used in the simulated experiments. Evaluating the model successively with increasing level of the target signal delivered its condition-specific psychometric function. The logarithmic d' as a function of target level is a straight line. The predicted detection threshold was obtained from a straight line fitted to the logarithmic d' .

3 Predictions of Binaural-Detection Datasets

In all experiments, a 500 Hz S_π or S_0 tone was to be detected in a broadband Gaussian noise masker. Figures 3, 4 and 5 show the experimental data denoted by symbols, as well as the predictions of the proposed model as continuous lines. Three types of binaural-detection experiments were simulated, as described in detail in the following subsections.

Table 1 summarizes the predicted experimental conditions.

3.1 van der Heijden & Trahiotis 1999

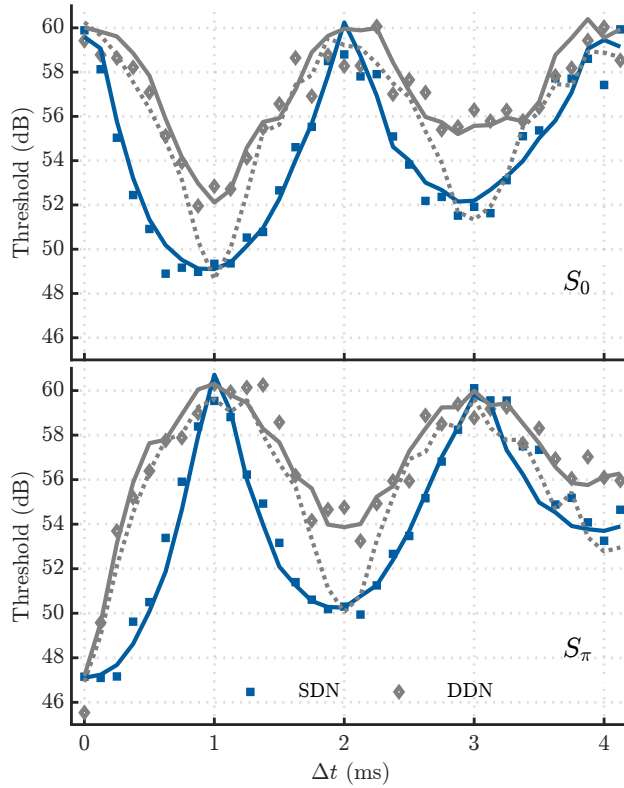


Figure 3: Experimental data from van der Heijden and Trahiotis (1999) (symbols). The continuous lines show the predictions of the presented model including the across-channel incoherence interference. The dashed lines show predictions for DDN with a single-channel version, i.e. without interference, equivalent to Encke and Dietz (2021). Upper panel: Detection thresholds with S_0 target; lower panel: with S_π target.

In this arguably most central experiment, detection thresholds of an S_0 target tone (Figure 3, upper panel) as well as of an S_π tone (Figure 3, lower panel) were measured as a function of the interaural masker delay, Δt , in steps of 0.125 ms. The bandwidth of the masker was 900 Hz. As outlined in the Introduction, the DDN consisted of two superimposed noises with opposite ITD. The experiment performed by van der Heijden and Trahiotis (1999) employed a four-interval, two-alternative forced choice task (4I-2AFC, first and fourth intervals always contained only the masker and served as queuing intervals). Their adaptive 2-down 1-up staircase procedure estimated the 70.7 % correct-response threshold. This is equivalent to a d' of 0.78 at threshold. The continuous lines in Figure 3 show the simulations of the presented model, including the across-channel incoherence interference. From visual inspection, the simulations captured all effects from the experimental thresholds and the critical threshold differences between SDN and DDN at all ITDs under

both conditions. Specifically, the critical 3 dB and 4 dB threshold difference at $\Delta t = 2$ ms in the S_π and $\Delta t = 1$ ms in the S_0 condition, respectively, are precisely accounted for. This good correspondence is also reflected in the more than 92 % explained variance under both conditions, and RMS errors of less than 1 dB. The dashed lines show simulations without the across-channel incoherence interference (single-channel version, equivalent to Encke and Dietz, 2021) but all other model parameters unchanged. This shows that a large amount of the threshold differences is already explained by differences in the on-frequency coherence. In much the same way as DDN coherence oscillates as a function of analysis frequency (Fig. 1c), it also fluctuates as a function of Δt . Particularly at $\Delta t = 0.5$ ms, DDN is incoherent in the 500-Hz band, whereas SDN is almost fully coherent. This, and not the across-frequency process, causes the difference in the simulated thresholds at this ITD. The across-frequency process only comes into play at those ITDs where the coherence at 500 Hz (on-frequency) is nearly identical in SDN and DDN (upper panel: $\Delta t = 1$ ms and 3 ms; lower panel: $\Delta t = 2$ ms and 4 ms).

3.2 Marquardt & McAlpine 2009

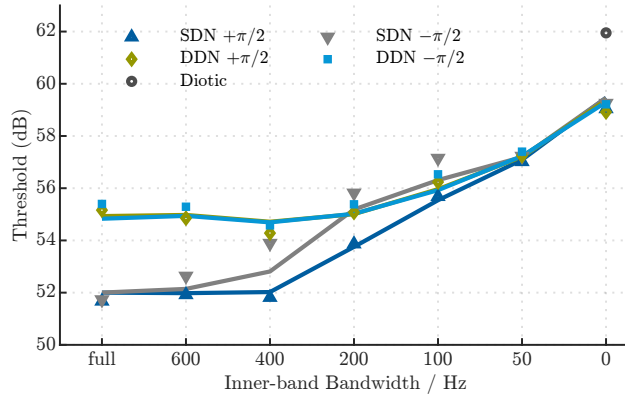


Figure 4: Experimental data from Marquardt and McAlpine (2009) (symbols) and model predictions (lines).

The stimuli of this experiment contained SDN or DDN centered at the frequency of the S_0 target tone with a constant Δt in the notch band. The notch was spectrally surrounded by constant-IPD bands with $\pi/2$ and $-\pi/2$, or vice versa. Thresholds are given as a function of the notch bandwidth. The resulting phase transitions between notch and flanking bands have been hypothesized to impair the detection if they cause a frequency region of low interaural coherence. The lower and upper frequency limits of the composite stimuli are 50 Hz and 950 Hz, respectively. The two-interval-two-alternative-forced choice task with a 3-down 1-up procedure that was used estimated the thresholds to be 79.4 % correct. This corresponds to $d' = 1.14$ at the threshold predicted by the model.

In Figure 4, detection thresholds of the S_0 tone are shown as a function of the bandwidth of the inner band. Again, the model predicted all critical characteristics of the data. These are the 3 dB at the full notch bandwidth (same as $\Delta t = 1$ ms in the S_0 condition in van der Heijden and Trahiotis 1999), the elevated SDN thresholds in the $[-\pi/2, \Delta t, +\pi/2]$ compared to the $[+\pi/2, \Delta t, -\pi/2]$ condition and the 3 dB BMLD where the notch bandwidth is zero.

3.3 Experiments on the operating bandwidth in binaural detection

Several studies investigated the operating bandwidth in binaural detection using notched-noise binaural detection (Sondhi and Guttman, 1966; Holube et al., 1998; Kolarik and Culling, 2010). The masking noise is diotic (N_0) in the notch band and antiphasic (N_π) in the flanking bands. Detection thresholds of an S_π target tone were again measured as a function of the notch bandwidth. Results are expressed as the difference between thresholds in the notched condition and the threshold without notch, i.e. $N_\pi S_\pi$. In Figure 5, the circles mark the threshold differences reported by Kolarik and Culling (2010, centered condition), which represent averages across their three participants. The triangles show individual thresholds of the two participants in the study by Holube et al. (1998, rectangular condition). The gray diamonds show the data from Sondhi and Guttman (1966). Our model predictions were oriented on the 2-down 1-up 2I-2AFC paradigm employed in Kolarik and Culling (2010), equivalent to $d' = 0.78$ at threshold. The black continuous line shows the model predictions with the same parameter settings as used to predict the S_π detection thresholds in van der Heijden and Trahiotis (1999, Figure 3b). The dotted black line shows model predictions without the across-channel interaction, so that detection was purely determined by the ERB = 79 Hz Gammatone filter centered at 500 Hz. Despite the large deviations between and within experiments, the model predictions involving the across-channel interaction captured the shape of the decreasing thresholds with increasing notch bandwidth.

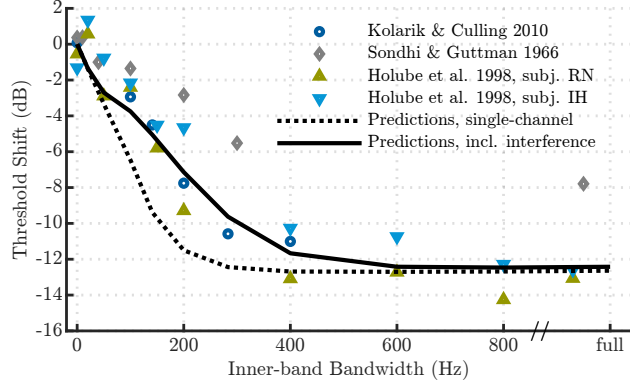


Figure 5: Symbols denote data from notched-noise binaural detection experiments with the configuration $N_{\pi 0\pi} S_{\pi}$ as a function of the inner-band (N_0) bandwidth; continuous line: Model prediction employing across-channel "incoherence"; dotted Line: Prediction with model relying only on the on-frequency filter (ERB = 79 Hz, centered at 500 Hz)

Experiment	Signal	Noise	Variable	$\hat{\rho}$	σ_b	σ_w	σ_m	Var. Exp./ %	RMSE / dB
van der Heijden and Trahiotis (1999)	π 0	$\pm \Delta t$	Δt	0.91 0.86	0.20 0.17	0.50 0.65	0.40 0.40	94.9 92.4	0.85 0.84
Marquardt and McAlpine (2009)	0	$[+\pi/2, \Delta t, -\pi/2]$ $[-\pi/2, \Delta t, +\pi/2]$ $[+\pi/2, \pm \Delta t, -\pi/2]$ $[-\pi/2, \pm \Delta t, +\pi/2]$	Δf	0.89	0.24	0.65	0.40	93.1 75.7 96.7 94.4	0.71 1.25 0.27 0.35
Kolarik and Culling (2010)	π	$[\pi, 0, \pi]$	Δf	0.91	0.20	0.50	0.40	97.1	0.67

Table 1: Summary of the simulated experiments and predictions. *Columns 1 - 4:* Simulated experiment, interaural configuration of the used target signal, that of the masking noise, independent variable (Δt : masker ITD; Δf : Masker inner-band bandwidth). *Columns 5 - 8:* Used model parameters: $\hat{\rho} < 1$: Maximum coherence (internal noise); σ_b : Standard deviation of the internal noise to determine the absolute performance of the binaural pathway; σ_w : Slope parameter of the double-exponential across-channel interaction window (normalized by the number of filters per ERB); σ_m : Standard Deviation of the level-dependent Internal Noise to determine the accuity of the monaural pathway; *Columns 9 - 10:* Percentage of the variance in the data accounted for by the model; Root Mean Squared Error of the predictions.

4 Discussion

It has been shown that a large amount of binaural detection data can be explained purely on the basis of the coherence $|\gamma|$ defined by a 79 Hz wide Gammatone filter at $f_c = 500$ Hz (Rabiner et al., 1966; Encke and Dietz, 2021). This accounts for experimentally obtained thresholds with fully coherent broadband noise maskers (Hirsh, 1948; van de Par and Kohlrausch, 1999), for mixtures of correlated and uncorrelated noise (Robinson and Jeffress, 1963; Pollack and Trittipoe, 1959; Bernstein and Trahiotis, 2014), and for experiments where interaural coherence is reduced by an ITD (Langford and Jeffress, 1964; Rabiner et al., 1966; Bernstein and Trahiotis, 2020). All these experiments have in common that the coherence and the phase relationship between noise and target are fairly constant across frequency bands. However, the on-frequency coherence does not account for thresholds obtained with maskers where these properties change substantially in filter bands that are relatively near to the target frequency. Specifically, the single-channel model version proposed in Encke and Dietz (2021) is not able to predict all of the threshold differences between SDN and DDN (see the dashed lines in Fig. 3).

Marquardt and McAlpine (2009) hypothesized across-channel processing in the binaural system to explain the reduced binaural benefit under such conditions. Here, we extended the analytical model by Encke and Dietz (2021) to a multi-channel numerical signal-processing model with interference of IPD fluctuations. With the interference applied only to the fluctuations, not the mean IPD, the proposed model differs from approaches assuming wider binaural filters (e.g. van der Heijden and Trahiotis, 1999; Kolarik and Culling, 2010). For stimuli with spectrally constant coherence and masker-target phase relations, e.g., SDN and all conditions simulated by Encke and Dietz (2021), the incoherence interference is moot and the model operates on the standard filter bandwidths of its peripheral filterbank.

The dataset of van der Heijden and Trahiotis (1999) contains both SDN and DDN, and is therefore the critical challenge

for binaural detection models¹. Their correlation-based model precisely predicted DDN detection thresholds by fitting the filter bandwidth to the data, such that the resulting correlation at $\tau = 0$ determined the DDN thresholds. The best-fitting peripheral filters had an ERB between 130 and 180 Hz at 500 Hz. The stronger unmasking with SDN was then attributed to ITD-compensating delay lines. Our model has the reverse rationale: The peripheral filter (ERB = 79 Hz) determines the coherence decline accounting for detection in SDN (Rabiner et al., 1966; Marquardt and McAlpine, 2009; Dietz et al., 2021; Encke and Dietz, 2021). The suggested interference mechanism then reduces the effective coherence in DDN (Marquardt and McAlpine, 2009), increasing detection thresholds. Both van der Heijden and Trahiotis' and our model simulate the data very accurately. Therefore, the discussion focuses on consequences and plausibility of the two different concepts.

The processing bandwidth dictates the temporal coherence and thus the decline of BMLD with increasing noise ITD in the absence of ITD compensation (Rabiner et al., 1966; van der Heijden and Trahiotis, 1999; Dietz et al., 2021). To date, two of the arguably most comprehensive datasets of dichotic tone-in-noise detection, van der Heijden and Trahiotis (1999) and Bernstein and Trahiotis (2020), have self-reported mutually exclusive requirements for the processing bandwidth (ERB = 130...180 Hz vs. ERB \leq 100 Hz at 500 Hz).

A variety of studies aims to estimate the binaural processing bandwidth by means of dichotic tone-in-noise detection, but no consistent picture emerges. There is, for example, a difference in estimated processing bandwidth between band-widening and notched-noise BMLD data, and between two different interaural configurations (e.g., Kolarik and Culling, 2010). Consequently, the topic is somewhat controversially debated and to date there is no clear consensus about either the underlying mechanism or the interpretation of the data (see, e.g., Verhey and van de Par, 2020 for review). Most of the recent binaural models, such as Bernstein and Trahiotis (2017) and Encke and Dietz (2021) assume a binaural processing bandwidth as narrow as the peripheral bandwidth. This is reasonable, considering direct measurements of the binaural processing bandwidth in ITD-sensitive inferior colliculus neurons in cats (Mc Laughlin et al., 2008): For (single) delayed noise, they found that damping of the cross-correlation function corresponds to the peripheral bandwidth at the respective center frequency. To develop a binaural model that also accounts for maskers that so far have been explained with a larger binaural processing bandwidth, like DDN, we built on the hypothesis of Marquardt and McAlpine (2009): We speculate that a low masker coherence in spectrally adjacent frequency bands reduces the ability of the auditory system to detect relatively smaller changes in IPD fluctuations caused by the target tone. This assumption, that listening is affected by the interaural incoherence in surrounding frequency regions, is related to binaural interference in detection tasks (Bernstein and Trahiotis, 1995) and to the more diffuse sound sensation. Hints towards across-channel processing in binaural unmasking were also found by Ewert et al. (2017), predicting spatial release from masking (SRM) with an equalization-cancellation (EC) model. Assuming an across-channel dependence of the EC parameters increased the predictive power. Conceptual similarity to the proposed across-channel incoherence interference can be found in models of monaural modulation processing: In Piechowiak et al. (2007) and Dau et al. (2013), modulation patterns interact across channels, while energetic spectral masking properties do not.

In contrast, in the case of narrow-band maskers, off-frequency channels can also improve $N_0 S_\pi$ detection, because they carry a similar signal-to-noise ratio van de Par and Kohlrausch (1999). The present single-channel detection stage does not exploit this effect (see Encke and Dietz 2021 for details), which is only a matter of the final d' integration stage (Breebaart et al., 2001b,c).

The binaural system's sensitivity to changes in ITD depends on the baseline ITD, including an IPD dependence for pure tones (Yost, 1974) and a reduced unmasking for $N_\pi S_0$ compared to $N_0 S_\pi$ Hirsh (1948). Delay-line models can account for this dependence with a corresponding $p(\tau)$ function. However, they then incorrectly predict better unmasking with $N_\pi S_0$ compared to $N_0 S_\pi$ when $\tau = T/2$ (Breebaart et al., 1999). The present model has a reversed problem and cannot

¹The most comprehensive simulation of dichotic tone in noise detection thresholds using a cross-correlation-based model is by Bernstein and Trahiotis (2017). It is not expected to simulate the DDN detection thresholds of van der Heijden and Trahiotis (1999) with a good accuracy, because an ERB of at least 130 Hz is necessary. Other DDN stimuli, used experimentally by Bernstein and Trahiotis (2015), were included in the model test battery by Bernstein and Trahiotis (2017). Those DDN stimuli, however, differed in several ways from the former. First, the target frequency is 250 Hz, compared to 500 Hz in van der Heijden and Trahiotis (1999) and in all other studies here simulated. Second, instead of fixing the target tone to S_0 or S_π , the target is delayed by the same amount as one of the two noises, i.e. $(N_0)_{\pm \Delta t} (S_\pi)_{\Delta t}$. Such an approach is useful for SDN, as it ensures a constant π difference between the IPDs of the noise and of the tone. For DDN, however, the IPD of the second noise relative to the tone is offset from π by $2\Delta t$. This type of stimulus therefore causes an even more complex Δt -dependence of threshold, which offers no advantage over the DDN from van der Heijden and Trahiotis (1999) for filter estimation. With both definitions, corresponding SDN and DDN stimuli can be generated only if Δt is an integer or a half-integer multiple of the target period (i.e. $\Delta t = n/2f$, $n \in \mathbb{N}$). In Bernstein and Trahiotis (2015) (their Figure 1, Panel a) these are the two data points at $\Delta t = 2$ and 4 ms. SDN and DDN thresholds are, however, very similar at those points. Third, the masker bandwidth is 50 Hz. For such a masker bandwidth similar to a peripheral filter width, neither van der Heijden and Trahiotis (1999) nor our model would predict a considerable threshold difference between SDN and DDN at $\Delta t = 2$ and 4 ms, since there are no off-frequency regions of considerably lower coherence.

account for the former difference. When accounting for the precision of IPD encoding from the Fisher information of neural response population recorded in mammals, this dependence is also expected (Harper and McAlpine, 2004; Encke, 2019). An angular compression of the decision variable space $\{\zeta\}$ at large IPD is a possible model extension. With the present implementation, the binaural pathway parameters $(\hat{\rho}, \sigma_b, \sigma_w)$ had to be adjusted slightly between conditions with S_π targets and conditions with S_0 targets (see Table 1).

5 Conclusion

The proposed binaural model with detrimental interaural incoherence interference operating across neighboring auditory filters simulates binaural detection thresholds from several data sets with spectrally complex maskers. Employing conventional auditory filters Glasberg and Moore (1990), it predicts the reduced unmasking in double-delayed noise (van der Heijden and Trahiotis, 1999) compared to conventional interaurally delayed noise. The concept can help to resolve the inconsistency inherent in the fact that binaural models require standard filter bandwidths for most data sets (Bernstein and Trahiotis, 2017, 2020), but at least 1.6 times wider filters for double-delayed noise van der Heijden and Trahiotis (1999) and other spectrally complex maskers Verhey and van de Par (2020). The main consequence of using a standard filter bandwidth is that the gradual decline of the binaural benefit with masker ITD can be simulated without internal ITD compensation, as first suggested by Langford and Jeffress (1964).

Acknowledgments

This work was funded by the Deutsche Forschungsgemeinschaft (DFG, German Research Foundation) – Projektnummer 352015383 – SFB 1330 B4.

A Derivation of cross-power spectral density in double-delayed noise

In DDN, two two-channel signals $u(t) = [u(t) \ u(t + \Delta t)]$ and $z(t) = [z(t) \ z(t - \Delta t)]$ with opposite ITDs, Δt and $-\Delta t$, are summed. The cross-power spectral density (CPSD) functions for ensembles of such signals are

$$\begin{aligned} S_{UU}(\omega) &= 0.5e^{i\Delta t \omega}, \\ S_{ZZ}(\omega) &= 0.5e^{-i\Delta t \omega}. \end{aligned} \quad (12)$$

The amplitudes are 0.5, so that a DDN has the same energy as a SDN. Summation of the time signals is equivalent to a summation of their CPSD functions, which leads to

$$S_{UZ} = S_{UU}(\omega) + S_{ZZ}(\omega) = \cos(\omega\Delta t). \quad (13)$$

This resulting cosine pattern is determined by the sum of the CPSDs' phases adding up or canceling each other at different frequencies. The modulus of this normalized CPSD $|C(\omega)|$ represents the coherent energy of the signals as a function of frequency (Gardner, 1992),

$$|C(\omega)| = \frac{|S_{UZ}(\omega)|}{\sqrt{S_{UU}(\omega)S_{ZZ}(\omega)}} = |\cos(\omega\Delta t)|. \quad (14)$$

If $|\gamma(\tau)|$ is based on ensembles of signals, then $|C(\omega)| = \mathcal{F}\{|\gamma(\tau)|\}$. As a continuous function of ω it gives a coherence for any frequency ω representing an infinitesimally small bandwidth $\Delta f \rightarrow 0$, illustrated as continuous lines in Figure 1c. The coherence for peripherally filtered, i.e. finite-bandwidth signals is an average of the frequencies' normalized CPSDs $|C(\omega)|$. The coherence decreases with increasing interaural delay Δt and increasing bandwidth Δf , as illustrated by the bars in Figure 1c. Two superimposed noises with Δt of ± 2 ms are in phase at 500 Hz. At 625 Hz, however, they have IPDs of $\Delta\varphi_1 = \pi/2$ and $\Delta\varphi_2 = -\pi/2$, respectively. The coherence between left and right signals at 625 Hz is therefore zero.

References

Ira J. Hirsh. The Influence of Interaural Phase on Interaural Summation and Inhibition. *The Journal of the Acoustical Society of America*, 20(4):536–544, July 1948. ISSN 0001-4966. doi:10.1121/1.1906407.

Ted L. Langford and Lloyd A. Jeffress. Effect of Noise Crosscorrelation on Binaural Signal Detection. *The Journal of the Acoustical Society of America*, 36(8):1455–1458, August 1964. ISSN 0001-4966. doi:10.1121/1.1919224.

Lawrence R. Rabiner, C. L. Laurence, and N. I. Durlach. Further Results on Binaural Unmasking and the EC Model. *The Journal of the Acoustical Society of America*, 40(1):62–70, July 1966. ISSN 0001-4966. doi:10.1121/1.1910065.

Donald E. Robinson and Lloyd A. Jeffress. Effect of Varying the Interaural Noise Correlation on the Detectability of Tonal Signals. *The Journal of the Acoustical Society of America*, 35(12):1947–1952, December 1963. ISSN 0001-4966. doi:10.1121/1.1918864.

Jörg Encke and Mathias Dietz. The complex correlation coefficient accounts for binaural detection. *in preparation*, 2021.

A. Khintchine. Korrelationstheorie der stationären stochastischen Prozesse. *Mathematische Annalen*, 109(1):604–615, December 1934. ISSN 1432-1807. doi:10.1007/BF01449156.

Brian R Glasberg and Brian C.J. Moore. Derivation of auditory filter shapes from notched-noise data. *Hearing Research*, 47(1-2):103–138, August 1990. ISSN 03785955. doi:10.1016/0378-5955(90)90170-T.

Lloyd A. Jeffress. A place theory of sound localization. *Journal of Comparative and Physiological Psychology*, 41(1):35–39, 1948. ISSN 0021-9940. doi:10.1037/h0061495.

Marcel van der Heijden and Constantine Trahiotis. Masking with interaurally delayed stimuli: The use of “internal” delays in binaural detection. *The Journal of the Acoustical Society of America*, 105(1):388–399, January 1999. ISSN 0001-4966. doi:10.1121/1.424628.

Richard M. Stern and Glenn D. Shear. Lateralization and detection of low-frequency binaural stimuli: Effects of distribution of internal delay. *The Journal of the Acoustical Society of America*, 100(4):2278–2288, October 1996. ISSN 0001-4966. doi:10.1121/1.417937.

Leslie R. Bernstein and Constantine Trahiotis. Effects of interaural delay, center frequency, and no more than “slight” hearing loss on precision of binaural processing: Empirical data and quantitative modeling. *The Journal of the Acoustical Society of America*, 144(1):292–307, July 2018. ISSN 0001-4966. doi:10.1121/1.5046515.

Leslie R. Bernstein and Constantine Trahiotis. A crew of listeners with no more than “slight” hearing loss who exhibit binaural deficits also exhibit higher levels of stimulus-independent internal noise. *The Journal of the Acoustical Society of America*, 147(5):3188–3196, May 2020. ISSN 0001-4966. doi:10.1121/10.0001207.

H. Steven Colburn. Theory of binaural interaction based on auditory-nerve data. II. Detection of tones in noise. *The Journal of the Acoustical Society of America*, 61(2):525–533, February 1977. ISSN 0001-4966. doi:10.1121/1.381294.

Man Mohan Sondhi and Newman Guttman. Width of the Spectrum Effective in the Binaural Release of Masking. *The Journal of the Acoustical Society of America*, 40(3):600–606, September 1966. ISSN 0001-4966. doi:10.1121/1.1910124.

Andrew J. Kolarik and John F. Culling. Measurement of the binaural auditory filter using a detection task. *The Journal of the Acoustical Society of America*, 127(5):3009–3017, May 2010. ISSN 0001-4966. doi:10.1121/1.3365314.

Mathias Dietz, Jörg Encke, Kristin I. Bracklo, and Stephan D. Ewert. Prediction of tone detection thresholds in interaurally delayed noise based on interaural phase difference fluctuations. *arXiv:2107.00320 [cs, eess]*, July 2021.

Torsten Marquardt and David McAlpine. Masking with interaurally “double-delayed” stimuli: The range of internal delays in the human brain. *The Journal of the Acoustical Society of America*, 126(6):EL177–EL182, December 2009. ISSN 0001-4966. doi:10.1121/1.3253689.

Marc Nitschmann and Jesko L. Verhey. Binaural notched-noise masking and auditory-filter shape. *The Journal of the Acoustical Society of America*, 133(4):2262–2271, April 2013. ISSN 0001-4966. doi:10.1121/1.4792352.

Inga Holube, Martin Kinkel, and Birger Kollmeier. Binaural and monaural auditory filter bandwidths and time constants in probe tone detection experiments. *The Journal of the Acoustical Society of America*, 104(4):2412–2425, October 1998. ISSN 0001-4966. doi:10.1121/1.423773.

Torsten Dau, Dirk Püschen, and Armin Kohlrausch. A quantitative model of the “effective” signal processing in the auditory system. I. Model structure. *The Journal of the Acoustical Society of America*, 99(6):3615–3622, June 1996. ISSN 0001-4966. doi:10.1121/1.414959.

Torsten Dau, Birger Kollmeier, and Armin Kohlrausch. Modeling auditory processing of amplitude modulation. I. Detection and masking with narrow-band carriers. *The Journal of the Acoustical Society of America*, 102(5):2892–2905, November 1997. ISSN 0001-4966. doi:10.1121/1.420344.

Morten L. Jepsen, Stephan D. Ewert, and Torsten Dau. A computational model of human auditory signal processing and perception. *The Journal of the Acoustical Society of America*, 124(1):422–438, July 2008. ISSN 0001-4966. doi:10.1121/1.2924135.

Jeroen Breebaart, Steven van de Par, and Armin Kohlrausch. Binaural processing model based on contralateral inhibition. I. Model structure. *The Journal of the Acoustical Society of America*, 110(2):1074–1088, August 2001a. ISSN 0001-4966. doi:10.1121/1.1383297.

Leslie R. Bernstein and Constantine Trahiotis. An interaural-correlation-based approach that accounts for a wide variety of binaural detection data. *The Journal of the Acoustical Society of America*, 141(2):1150–1160, February 2017. ISSN 0001-4966. doi:10.1121/1.4976098.

Thomas Biberger and Stephan D. Ewert. Envelope and intensity based prediction of psychoacoustic masking and speech intelligibility. *The Journal of the Acoustical Society of America*, 140(2):1023–1038, August 2016. ISSN 0001-4966. doi:10.1121/1.4960574.

V. Hohmann. Frequency analysis and synthesis using a Gammatone filterbank. *Acta Acustica united with Acustica*, 88(3):433–442, May 2002.

Mathias Dietz and Go Ashida. Computational Models of Binaural Processing. In Ruth Y. Litovsky, Matthew J. Goupell, Richard R. Fay, and Arthur N. Popper, editors, *Binaural Hearing*, volume 73, pages 281–315. Springer International Publishing, Cham, 2021. ISBN 978-3-030-57099-6 978-3-030-57100-9. doi:10.1007/978-3-030-57100-9_10.

David McAlpine, Dan Jiang, and Alan R. Palmer. A neural code for low-frequency sound localization in mammals. *Nature Neuroscience*, 4(4):396–401, April 2001. ISSN 1546-1726. doi:10.1038/86049.

Benedikt Grothe, Michael Pecka, and David McAlpine. Mechanisms of Sound Localization in Mammals. *Physiological Reviews*, 90(3):983–1012, July 2010. ISSN 0031-9333, 1522-1210. doi:10.1152/physrev.00026.2009.

Ida Siveke, Stephan D. Ewert, Benedikt Grothe, and Lutz Wiegreb. Psychophysical and Physiological Evidence for Fast Binaural Processing. *Journal of Neuroscience*, 28(9):2043–2052, February 2008. ISSN 0270-6474, 1529-2401. doi:10.1523/JNEUROSCI.4488-07.2008.

Philip X. Joris, Bram Van de Sande, Dries H. Louage, and Marcel van der Heijden. Binaural and cochlear disparities. *Proceedings of the National Academy of Sciences*, 103(34):12917–12922, August 2006. ISSN 0027-8424, 1091-6490. doi:10.1073/pnas.0601396103.

Marcel van der Heijden and Philip X. Joris. Interaural Correlation Fails to Account for Detection in a Classic Binaural Task: Dynamic ITDs Dominate N0S π Detection. *Journal of the Association for Research in Otolaryngology*, 11(1):113–131, March 2010. ISSN 1525-3961, 1438-7573. doi:10.1007/s10162-009-0185-8.

Mohamed Bingabr, Blas Espinoza-Varas, and Philipos C. Loizou. Simulating the effect of spread of excitation in cochlear implants. *Hearing Research*, 241(1-2):73–79, July 2008. ISSN 03785955. doi:10.1016/j.heares.2008.04.012.

Jan Dirk Biesheuvel, Jeroen J. Briaire, and Johan H. M. Frijns. A Novel Algorithm to Derive Spread of Excitation Based on Deconvolution. *Ear & Hearing*, 37(5):572–581, September 2016. ISSN 0196-0202. doi:10.1097/AUD.0000000000000296.

Quinn McNemar. *Psychological Statistics*. Wiley, New York, 4th ed edition, 1969. ISBN 978-0-471-58708-8.

Helge Lüddemann, Helmut Riedel, and Birger Kollmeier. Logarithmic Scaling of Interaural Cross Correlation: A Model Based on Evidence from Psychophysics and EEG. In Birger Kollmeier, Georg Klump, Volker Hohmann, Ulrike Langemann, Manfred Mauermann, Stefan Uppenkamp, and Jesko Verhey, editors, *Hearing – From Sensory Processing to Perception*, pages 379–388, Berlin, Heidelberg, 2007. Springer. ISBN 978-3-540-73009-5. doi:10.1007/978-3-540-73009-5_41.

Dieter Just and Richard Bamler. Phase statistics of interferograms with applications to synthetic aperture radar. *Applied Optics*, 33(20):4361, July 1994. ISSN 0003-6935, 1539-4522. doi:10.1364/AO.33.004361.

A. J. Simpson and M. J. Fitter. What is the best index of detectability? *Psychological Bulletin*, 80(6):481–488, 1973. ISSN 0033-2909. doi:10.1037/h0035203.

John A. Swets. Form of empirical ROCs in discrimination and diagnostic tasks: Implications for theory and measurement of performance. *Psychological Bulletin*, 99(2):181–198, 1986. ISSN 1939-1455(Electronic),0033-2909(Print). doi:10.1037/0033-2909.99.2.181.

Stephan D. Ewert and Torsten Dau. Characterizing frequency selectivity for envelope fluctuations. *The Journal of the Acoustical Society of America*, 108(3):1181, 2000. ISSN 00014966. doi:10.1121/1.1288665.

Shigeto Furukawa. Detection of combined changes in interaural time and intensity differences: Segregated mechanisms in cue type and in operating frequency range? *The Journal of the Acoustical Society of America*, 123(3):1602–1617, March 2008. ISSN 0001-4966. doi:10.1121/1.2835226.

Michael J. Hacker and Roger Ratcliff. A revised table of d' for M-alternative forced choice. *Perception & Psychophysics*, 26(2):168–170, 1979. ISSN 1532-5962(Electronic),0031-5117(Print). doi:10.3758/BF03208311.

Steven van de Par and Armin Kohlrausch. Dependence of binaural masking level differences on center frequency, masker bandwidth, and interaural parameters. *The Journal of the Acoustical Society of America*, 106(4):1940–1947, October 1999. ISSN 0001-4966. doi:10.1121/1.427942.

Irwin Pollack and W. J. Trittipoe. Binaural Listening and Interaural Noise Cross Correlation. *The Journal of the Acoustical Society of America*, 31(9):1250–1252, September 1959. ISSN 0001-4966. doi:10.1121/1.1907852.

Leslie R. Bernstein and Constantine Trahiotis. Accounting for binaural detection as a function of masker interaural correlation: Effects of center frequency and bandwidth. *The Journal of the Acoustical Society of America*, 136(6): 3211–3220, December 2014. ISSN 0001-4966. doi:10.1121/1.4900830.

Leslie R. Bernstein and Constantine Trahiotis. Converging measures of binaural detection yield estimates of precision of coding of interaural temporal disparities. *The Journal of the Acoustical Society of America*, 138(5):EL474–EL479, November 2015. ISSN 0001-4966. doi:10.1121/1.4935606.

Jesko L. Verhey and Steven van de Par. Binaural frequency selectivity in humans. *European Journal of Neuroscience*, 51(5):1179–1190, March 2020. ISSN 0953-816X, 1460-9568. doi:10.1111/ejn.13837.

Myles Mc Laughlin, Joelle Nsimire Chabwine, Marcel van der Heijden, and Philip X. Joris. Comparison of Bandwidths in the Inferior Colliculus and the Auditory Nerve. II: Measurement Using a Temporally Manipulated Stimulus. *Journal of Neurophysiology*, 100(4):2312–2327, October 2008. ISSN 0022-3077. doi:10.1152/jn.90252.2008.

Leslie R. Bernstein and Constantine Trahiotis. Binaural interference effects measured with masking-level difference and with ITD- and IID-discrimination paradigms. *The Journal of the Acoustical Society of America*, 98(1):155–163, July 1995. ISSN 0001-4966. doi:10.1121/1.414467.

Stephan D. Ewert, Wiebke Schubotz, Thomas Brand, and Birger Kollmeier. Binaural masking release in symmetric listening conditions with spectro-temporally modulated maskers. *The Journal of the Acoustical Society of America*, 142(1):12–28, July 2017. ISSN 0001-4966. doi:10.1121/1.4990019.

Tobias Piechowiak, Stephan D. Ewert, and Torsten Dau. Modeling comodulation masking release using an equalization-cancellation mechanism. *The Journal of the Acoustical Society of America*, 121(4):2111–2126, April 2007. ISSN 0001-4966. doi:10.1121/1.2534227.

Torsten Dau, Tobias Piechowiak, and Stephan D. Ewert. Modeling within- and across-channel processes in comodulation masking release. *The Journal of the Acoustical Society of America*, 133(1):350–364, January 2013. ISSN 0001-4966. doi:10.1121/1.4768882.

Jeroen Breebaart, Steven van de Par, and Armin Kohlrausch. Binaural processing model based on contralateral inhibition. II. Dependence on spectral parameters. *The Journal of the Acoustical Society of America*, 110(2):1089–1104, August 2001b. ISSN 0001-4966. doi:10.1121/1.1383298.

Jeroen Breebaart, Steven van de Par, and Armin Kohlrausch. Binaural processing model based on contralateral inhibition. III. Dependence on temporal parameters. *The Journal of the Acoustical Society of America*, 110(2):1105–1117, August 2001c. ISSN 0001-4966. doi:10.1121/1.1383299.

William A. Yost. Discriminations of interaural phase differences. *The Journal of the Acoustical Society of America*, 55 (6):1299–1303, June 1974. ISSN 0001-4966. doi:10.1121/1.1914701.

Jeroen Breebaart, Steven van de Par, and Armin Kohlrausch. The contribution of static and dynamically varying ITDs and IIDs to binaural detection. *The Journal of the Acoustical Society of America*, 106(2):979–992, August 1999. ISSN 0001-4966. doi:10.1121/1.427110.

Nicol S. Harper and David McAlpine. Optimal neural population coding of an auditory spatial cue. *Nature*, 430(7000): 682–686, August 2004. ISSN 1476-4687. doi:10.1038/nature02768.

Jörg Encke. *A Model of the Neuronal Representation of Interaural Phase Differences*. Dissertation, Technische Universität München, München, 2019.

William A. Gardner. A unifying view of coherence in signal processing. *Signal Processing*, 29(2):113–140, November 1992. ISSN 01651684. doi:10.1016/0165-1684(92)90015-O.